의학박사 학위논문

Various mRNA expressions in uterus of ovariectomized cyclophosphamide-treated mice according to estradiol injection and resting time

난소 제거 후 사이클로포스파마이드 투여 마우스의 자궁에서 에스트라디올 주입 및 휴식기 시간에 따른 다양한 mRNA 발현 양상

2021년 08월

서울대학교 대학원

의학과 산부인과학전공

김 자 연

Various mRNA expressions in uterus of ovariectomized cyclophosphamide-treated mice according to estradiol injection and resting time

난소 제거 후 사이클로포스파마이드 투여 마우스의 자궁에서 에스트라디올 주입 및 휴식기 시간에 따른 다양한 mRNA 발현 양상

지도교수 지병철

이 논문을 의학박사 학위논문으로 제출함

2021년 6월

서울대학교 대학원

의학과 산부인과학전공

김 자 연

김자연의 박사 학위논문을 인준함

2021년 6월

위 원 장 _____

부위원장 _____

위 원 _____

위 원 _____

위 원 _____

Abstract

Expressions of various mRNAs in uterus of ovariectomized cyclophosphamide-treated mice according to estradiol injection and resting time

Jayeon Kim

College of Medicine

The Department of Obstetrics & Gynecology

The Graduate School

Seoul National University

AIM: To investigate 1) histologic change of reproductive organs and their fertility in cyclophosphamide (CYP)-treated mice 2) expressions of various mRNAs in uterus of ovariectomized CYP-treated mice according to estradiol injection and resting time.

METHODS: Seven-week-old C57BL/6 female mice were used and CYP was injected six times via intraperitoneal route (3 mg each at day 0, 2, 4, 6, 8, and 10). In experiment 1, female mice were sacrificed at day 11 and morphology and histology of various organs were analyzed. A part of female mice was mated with fertile males at day 16 and then pregnancy was checked.

In experiment 2, female mice were ovariectomized at day 0 and CYP was injected six times as the above schedule (OVX-CYP model). At day 18 (OVX-CYP-one-week-rest model) and day 24 (OVX-CYP-two-week-rest model), 0.1 mg of estradiol (E) was injected subcutaneously and then mice were sacrificed 0, 2, 6, or 24 hours later. OVX-saline model was used as control. After obtaining uterine tissues at each time, various mRNAs were assayed by RNA-seq, reverse transcription-PCR (RT-PCR), and real-time RT-PCR.

RESULTS: In experiment 1, overall atrophy of uterus and endometrium was observed after CYP injection. Ovaries were also atrophied and the number of ovarian follicles was significantly decreased compared to saline control. After mating, the time to plug formation was significantly increased in the CYP-treated mice, and they did not give birth until 20 days after plug formation.

In experiment 2, increased uterine expression of mRNAs related to immune response, cell death, and stress response was observed in the OVX-CYP-one-week-rest model, irrespective of E injection, but immune response-related mRNAs were decreased in the OVX-CYP-two-week-rest model.

Uterine expression of upregulated or downregulated E-responsive mRNAs were markedly altered in OVX-CYP-one-week-rest model, irrespective of E treatment, but all of those mRNAs were restored in the OVX-CYP-two-week-rest model.

CONCLUSION: CYP injection induced overall atrophy of uterus and

endometrium and decreased the number of ovarian follicle, and further, severely hampered fertility in female mice. CYP injection into ovariectomized mice and one-week of resting induced markedly alteration of several uterine mRNAs expression, irrespective of E injection, but those were restored successfully after two-week of resting. These findings suggest that altered uterine mRNA expression by CYP injection could be reversible after two-week of resting, but not by E injection.

Keywords: cyclophosphamide; ovary; fertility; uterus, endometrium, estrogen

Student number: 2015-30567

Table of Contents

List of table

List of figures

Chapter 1. Introduction

1.1. Study Background

As a result of the high survival rates and the growing emphasis on the cancer survivor' s quality of life, there has been increased attention to the issue of fertility preservation (FP).[1,2]

As growing number of female patients with cancer pursue FP such as oocyte, embryo or ovarian tissue cryopreservation, increasing number of patients return to use their frozen gametes for a successful pregnancy after the cessation of cancer treatment. Therefore, the researches about the optimal timing and condition for utilization of frozen gametes in cancer survivors are warranted.

So far, most researches about fertility preservation have focused on damage to gametes including oocytes and sperm. However, the damage to gametes and ovaries can be offset, although partially, by cryopreservation of gametes before cancer treatment.

Importantly, there is lack of studies investigating the uterine damage and recovery after gonadotoxic chemotherapy.

One recent study showed comparable pregnancy rate using frozen embryo in women with breast cancer to those expected in a non-cancer population undergoing in vitro fertilization.[3]

On the contrary, lower implantation rate was reported in oocyte

donation cycles in cancer survivors who had had a history of chemotherapy and/or radiotherapy.[4]

It was also reported that, women who had received chemotherapy had a higher risk of preterm birth which was limited to those survivors who had short intervals between treatment and conception.[5]

However, so far, there is no study showing a direct uterine damage by chemotherapy.

The results from studies regarding the impact of chemotherapy on uterus is complicated. Uterus is regulated by the ovarian sex steroid hormones throughout the menstrual cycle. It is clinically critical whether the undesired effect of chemotherapy on uterus is indirectly mediated by ovarian damage or is directly induced by chemotherapy itself.

A recent study showing a favorable pregnancy rate using frozen embryo after chemotherapy may imply that uterine damage by chemotherapy occurs indirectly through ovarian damage which can be overcome by hormonal replacement.[3]

However, in an animal study investigating mRNA expression and activity of topoisomerase I activity in endometrium, anticancer drug (camptothecin) severely impair directly endometrial integrity and receptivity.[6]

1.2. Purpose of Research

The aim of this study was to investigate 1) histologic change of reproductive organs and their fertility in cyclophosphamide (CYP)-treated mice and 2) various mRNA expressions in the uterus of ovariectomized CYP-treated mice according to estradiol (E) injection and resting time.

Chapter 2. Materials and Methods

2.1. Study animals

All mice used in this study were maintained in accordance with the policies of the CHA University Institutional Animal Care and Use Committee (IACUC, No180178). Seven-week-old (adult) C57BL/6 female mice were provided by Orient Bio (Gapyeong, Gyeonggi, Korea). Four to eight mice were included at each experiment set

2.2. Experimental Design: CYP and estradiol treatment

CYP and E were purchased from Sigma-Aldrich (St. Louis, MO, USA). All mice were housed until they weighed more than 20g to increase survival rate after CYP administration.

In experiment 1, 3 mg of CYP was injected six times via intraperitoneal route (at day 0, 2, 4, 6, 8, and 10) (Fig. 1A) and the body weight and survival rate was assessed. Female mice were sacrificed at day 11 and gross morphology and histology of various organs were analyzed. A part of female mice was mated with fertile males at day 16 and then pregnancy was checked (Fig. 2A). In experiment 1, mice with 0.1 mL of saline injection were used as control (saline control).

In experiment 2, female mice were ovariectomized at day 0 and 3 mg of CYP was injected six times as the above schedule (OVX-CYP

model). At day 18 (OVX-CYP-one-week-rest model), 0.1 mg of E was injected subcutaneously and then mice were sacrificed at 0, 2, 6, or 24 hours post-E (Fig. 3A). At day 24 (OVX-CYP-two-week-rest model), 0.1 mg of E was injected subcutaneously and then mice were sacrificed at 0, 2, 6, or 24 hours post-E (Fig. 5A). In experiment 2, ovariectomized mice with 0.1 mL of saline injection were used as control (OVX-saline model).

2.3. Hematoxylin and eosin staining

Uterus, ovary, heart, kidney, stomach and spleen were dissected, and then fixed in 4% paraformaldehyde for histology. Fixed tissues were washed, dehydrated, and embedded in Paraplast (Merck KGaA, Darmstadt, Germany). Paraffin-embedded tissues were cut at 5 μm in thickness using a microtome and stained with Hematoxylin and Eosin (H&E) (Sigma-Aldrich).

2.4. mRNA sequencing and data analysis

Quant-3' mRNA-seq. was initially performed using 2 μg of total RNA (n = 1 pool per group; 3-4 mice per pool; Ebiogen, Seoul, Korea). mRNAs were used for the cDNA synthesis and shearing, following the manufacture's instruction. Indexing was performed using the Illumina indexes. The enrichment step was carried out using PCR. Subsequently, libraries were checked using the Agilent

2100 bioanalyzer (DNA High Sensitivity Kit) to evaluate the mean fragment size.

Quantification was performed via the library quantification kit using a StepOne Real-Time PCR System (Life Technologies, Inc., USA). RNA-Seq reads were mapped using the TopHat software tool in order to obtain the (ref: alignment file How to map billions of short reads onto genomes). Differentially expressed genes were determined based on counts from unique and multiple alignments using coverage in Bedtools.[7]

The Read Count data were processed based on the Quantile normalization method using EdgeR within R using Bioconductor. The alignment files also were used for assembling transcripts, estimating their abundances, and detecting differential expression of genes or isoforms using cufflinks. Additionally, we used the FPKM (fragments per kilobase of exon per million fragments) as the method of determining the expression level of the gene regions. Gene classification was based on searches performed using GSEA software (Gene Set Enrichment Analysis) and QuickGO (https://www.ebi.ac.uk/QuickGO/).

2.5. RNA extraction, reverse transcription-PCR (RT-PCR), and real-time RT-PCR

Uterine tissues at each experiment set were obtained and vitrified.

After warming, total RNA was extracted by using Trizol Reagent (Invitrogen life technologies, San Diego, CA, USA) according to the manufacturer' s protocols. cDNA was synthesized from 1 μg of total RNA by using M-MLV reverse transcriptase (Promega, Madison, Wisconsin, USA) and RNasin Ribonuclease inhibitor (Promega). Synthesized cDNA was utilized for real-time RT-PCR with specific primers (Table 1) at optimized primer melting temperature (Tm). Real-time RT-PCR was performed by using iQTM SYBR Green Supermix (Bio-Rad, Hercules, CA, USA) on BIO-RAD iCycler. Standard curve of cycle thresholds for several serial dilutions of a cDNA sample was established and then used to calculate the relative abundance of each gene. *rPL7* was used as a reference gene in all the experiments. All PCR reactions were performed in duplicate.

Table 1. Primer sequences for real-time RT-PCR

Gene		Sequence
s100a8	F	TTGATGTCTACCACAATTATTCCAATAT
	R	CCAATTCTCTGAACAAGTTTTCG
s100a9	F	CGACACCTTCCATCAATACTCTAG
	R	GCTGATTGTCCTGGTTTGTG
Camp	F	TGGTGAAGCAGTGTATGGG
	R	CCAGCCGGGAAATTTTCTTG
Bcl7b	F	AAGAAATGGGTGACTGTGGG
	R	GCTCTGGTTGCTGTTCTCATC
Cdkn1a	F	GACAAGAGGCCCAGTACTTC
	R	AATCTGCGCTTGGAGTGATAG
Cstb	F	GATCTGTCTTCAGCTTCTCCG
	R	GCCACTATCTGTCTCTTGAAGG
Atf5	F	GCTCACACCGTCTCTTCAG
	R	CAGCGTGGAAGATTGTTCAG
Pdcd6ip	F	GTCCCTGGCTGTGTTTAGTC
	R	GATGCCTCCCTGTTCAACTAC
Dcn	F	AGTGTTCTGATCTGGGTTTGG
	R	TCACGAGAGGTTTGAATGCC
Serping1	F	TCGATGACCATACTTTGAAGGC
	R	AGGTAAGTGGGCAGGAATTTG
Il15	F	CCTTAAGAACACAGAAACCCATG
	R	AGGAAACACAAGTAGCACGAG
Bach2	F	CTGTAGCCTTCTCATCTCTTCC
	R	TCTTCCGTTGGTCATTGAGG

2.6. Statistical analysis

Statistical analyses were performed using the unpaired Student' s t−tests and $p < 0.05$ was considered statistically significant. All values represent the mean ± standard deviation. The expression level of mRNA was described as a relative amount to control group (saline control).

Chapter 3. Results

2.1. Body weight loss in CYP-treated mice and evaluation of gross morphology and histology of various organs

To validate the optimal experimental dose of CYP, 3 mg, 4 mg, or 5 mg of CYP was injected and dose-dependent actions of CYP on the body weight and survival rate was assessed. In the CYP-treated mice, there was a significant body weight loss, compared to saline control group, and body weight loss was more severe as the dose of CYP increased (Fig. 1B).

In terms of survival rate, all mice survived after 3 mg of CYP, but survival rate rapidly dropped after 4 mg and 5 mg of CYP injection (Fig. 1C).

Therefore, we used 3 mg of CYP in all followed experiments.

Fig. 1D shows representative gross body shape of mice after saline or 3 mg of CYP.

Between mice after saline or 3 mg of CYP-treated mice, the weight of heart and histologic examination was similar (Fig. 1E). However, the weight of kidney was reduced, and the weight of stomach and spleen were increased and abnormally enlarged.

Histologic examination of kidney and stomach revealed no definite change after CYP administration (Fig. 1F).

In particular, histologic examination of spleen revealed that the white pulp appeared to be atrophic overall and the boundaries of the white pulp (a lymphoid tissue composed of lymphocytes) could not be distinguished (Fig. 1G).

Gross examination revealed that the uterus was severely atrophied in the CYP-treated mice, compared to saline control (Fig. 1H).

Microscopically, uterus was severely atrophied and ovaries were also severely atrophied; there was significantly less ovarian follicles in the CYP-treated mice (Fig. 1I).

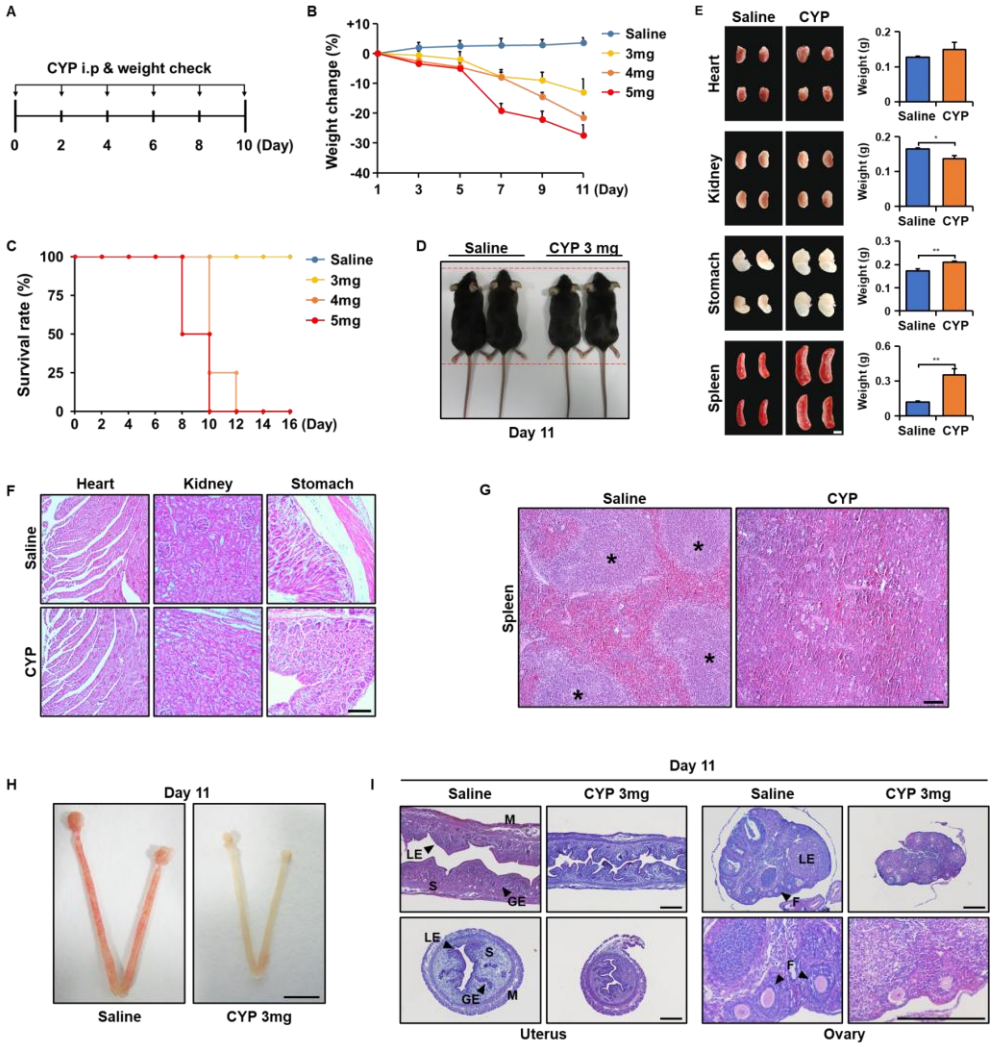

Figure 1. Gross and histological examinations in cyclophosphamide (CYP)-treated mice.

(A) Schedule for CYP (3 mg, 4 mg, or 5 mg) or saline (0.1 mL) injection via intraperitoneal (i.p) and body weight measurement. Injection was performed day 0, 2, 4, 6, 8, and 10 (total six times), and mice were killed day 11.

(B) Changes in percentage of body weight relative to initial body weight on day 1 through day 11 (n = 6 per each group).

(C) Survival rate according to dose of CYP (3 mg, 4 mg, 5 mg) (n = 4 to 8 per each group).

(D) Representative whole-body photography of saline control and 3 mg of CYP

injection mice at day 11.

(E) Gross morphology and weight of various organs (heart, kidney, stomach, and spleen) in saline control and 3 mg of CYP injection mice at day 11 (n = 5 per each group). Scale bar: 5 mm.

(F) Histological analyses of heart, kidney, and stomach in saline control and 3 mg of CYP injection mice at day 11. Scale bar: 100 μm.

(G) Histological analyses of spleen in saline control and 3 mg of CYP injection mice at day 11. Scale bar: 100 μm. *indicates white pulp.

(H) Gross morphology of uterus in saline control and 3 mg of CYP injection mice at day 11. Scale bar: 5 mm.

(I) Histological analyses of uterus and ovary in saline control and 3 mg of CYP injection mice at day 11. Scale bar: 400 μm. GE, Glandular epithelium; LE, Luminal epithelium; S, Stroma; M, Myometrium; CL, Corpus luteum; F, follicle. Unpaired Student's t-test, *$p<0.05$, **$p<0.01$.

3.2. Fertility in CYP-treated mice

CYP-treated mice were mated male mice at day 16 (Fig. 2A).

The body weight of CYP-treated mice was decreased during multiple CYP injections, but was stable during rest period (until day 17) (Fig. 2B).

The time to plug confirmation after mating was significantly increased in the CYP-treated mice, compared with saline control, and the pregnancy rate was significantly decreased (Fig. 2C-E).

When the second pregnancy was induced, the time to plug confirmation after mating was similar between the CYP-treated mice and saline control, but the CYP-treated mice failed to give birth (Fig. 2F-H).

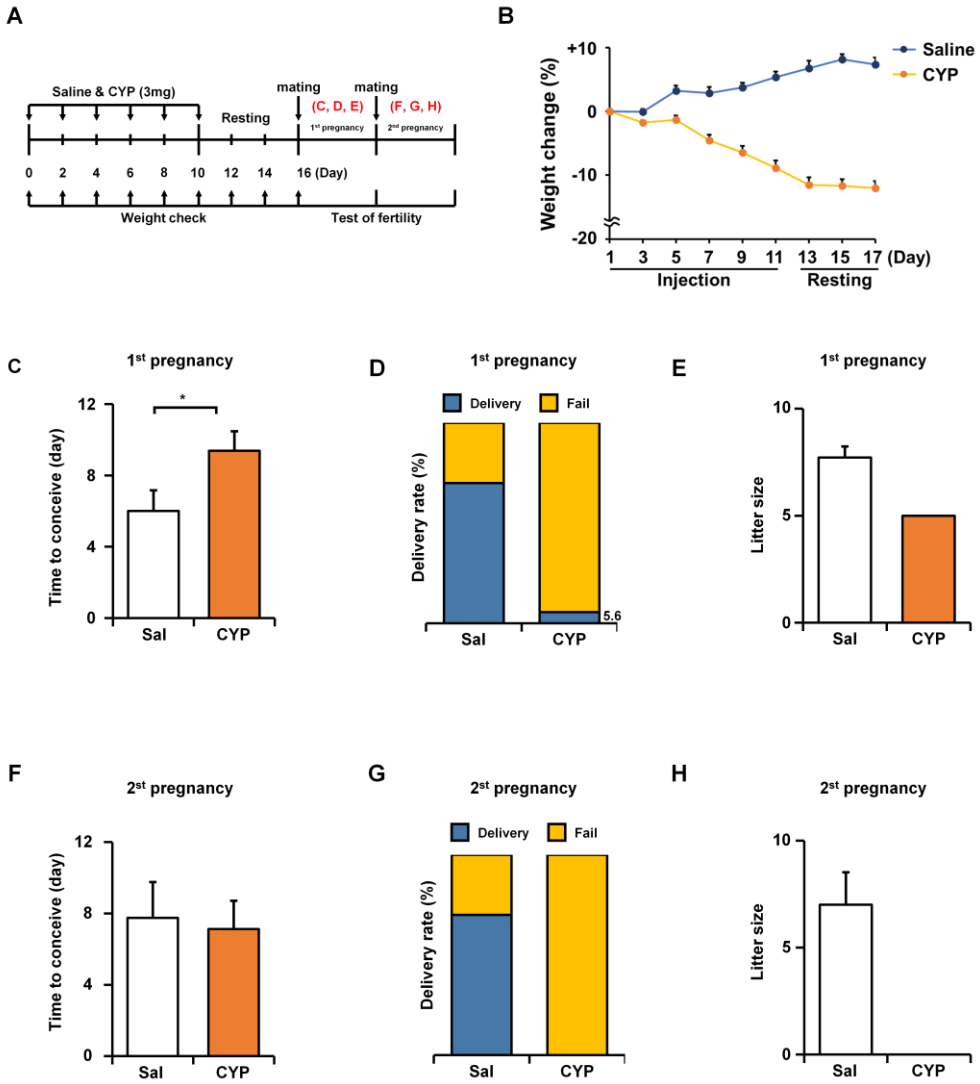

Figure 2. Fertility test in in saline control and 3 mg of CYP-treated mice.

(A) Schedule for 3 mg of CYP or saline (0.1 mL) injection via intraperitoneal (i.p) and body weight measurement. Injection was performed day 0, 2, 4, 6, 8, and 10 (total six times), and mice were mated with fertile males at day 16.

(B) Change in percentage of body weight relative to initial body weight on day 1 through day 17 (n = 10-18 per each group).

(C) The mean time to plug confirmation by first pregnancy.

(D) Delivery rate by first pregnancy.

(E) The mean of litter size by first pregnancy.

(F) The mean time to plug confirmation by second pregnancy.

(G) Delivery rate by second pregnancy. #CYP-treated mice did not give birth.

(H) The mean of litter size by second pregnancy (in saline control only).

Unpaired Student's t-test, *$p < 0.05$.

3.3. Uterine expression of various mRNAs in OVX-CYP-one-week-rest model

To investigate the direct effect of CYP on the uterus (i.e. independent from ovary), OVX-CYP-one-week-rest model was established (Fig. 3A).

By using uterine tissues in the OVX-CYP-one-week-rest model, mRNA-seq. was performed to elucidate possible mRNA changes after 3 mg of CYP injection.

Table 2 shows top 10 upregulated mRNAs out of 7,430 mRNAs in OVX-CYP-one-week-rest model relative to OVX-saline control. Among them, five mRNAs were related with immune response, two mRNAs were related with leukocyte, two mRNAs were related with cell death, and one mRNA was related with stress response (Fig. 3B&C).

Among seven immune response-related mRNAs, we confirmed that the expression of *s100a8*, *s100a9*, and *Cam* was highly increased in the OVX-CYP-one-week-rest model (Fig. 3D&E). The individual relative expression levels of these three mRNAs were depicted in Fig. 3F.

Table 2. Gene ontology (GO) enrichment analysis for top 10 upregulated uterine mRNAs in OVX-CYP-one-week model.

Rank	Name	Size	NES	FDR q-val
1	Myeloid leukocyte activation	73	3.05	0
2	Myeloid leukocyte mediated immunity	62	3.02	0
3	Tertiary granule	24	2.88	0
4	Leukocyte mediated immunity	81	2.78	1.7E-04
5	Specific granule	28	2.80	2.0E-04
6	Cell activation involved in immune response	74	2.84	2.5E-04
7	Specific granule lumen	16	2.66	7.9E-04
8	Specific granule	81	2.65	8.1E-04
9	Positive regulation of reactive oxygen species metabolic process	18	2.66	8.9E-04
10	Defense response to bacterium	29	2.66	0.0010

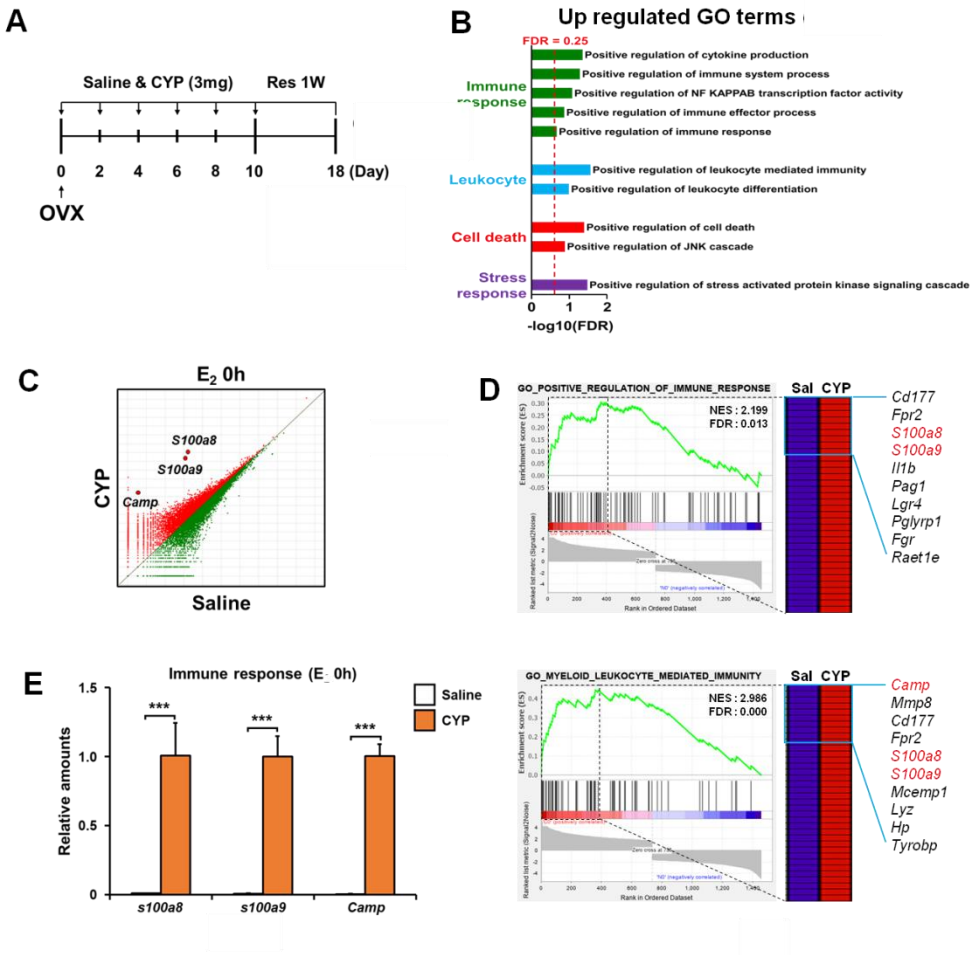

Figure 3. Searching upregulated gene sets via mRNA seq. and GSEA analysis in the uterus of OVX-CYP-one-week model. All expression levels in OVX-CYP-one-week model were assessed by relative expression to OVX-saline control.

(A) Schedule for 3 mg of CYP or saline (0.1 mL) injection via intraperitoneal (i.p). Injection was performed day 0, 2, 4, 6, 8, and 10 (total six times), and mice were killed at day 18.

(B) Top 10 upregulated uterine mRNAs in OVX-CYP-one-week model (unsupervised hierarchical clustering).

(C) Scatterplot analysis from mRNA-seq. peaks in OVX-CYP-one-week model and OVX-saline control.

(D) Two representative diagrams from GSEA to identify upregulated GO terms in

OVX-CYP-one-week model. Gene sets with an FDR q-value < 0.25 (red dotted line) were considered significant.

(E) Expression level of three immune response-related mRNAs (*s100a8*, *s100a9*, and *Camp*) by real-time RT-PCR (normalized read count, log2) (n = 3-5 per group). Unpaired Student' s t-test, ***p <0.005.

3.4. Expression of immune response-related mRNAs and E-responsive mRNAs in OVX-CYP-one-week-rest model and OVX-saline control after E treatment

In the OVX-CYP-one-week-rest model and OVX-saline control, 0.1 mg of E was injected subcutaneously at day 18 and then mice were sacrificed at 0, 2, 6, or 24 hours post-E (Fig. 4A).

Fig. 4B shows several upregulated mRNAs at four time points after E injection, and they were mostly immune response-related. The expressions of immune response-related mRNAs were generally decreased in time-dependent manner after E injection.

The non-hierarchical clustering analysis showed that the uterine expression pattern of mRNAs after E injection was quite different between the OVX-CYP-1-week-rest and OVX-saline control at each four time points (Fig. 4C).

Especially, the expression level of *s100a8*, *s100a9*, and *Cam* in the OVX-CYP-1-week-rest model were always significantly higher than OVX-saline control (Fig. 4D). However, throughout four time points, their expression levels were not changed either in the OVX-CYP-1-week-rest model or OVX-saline control.

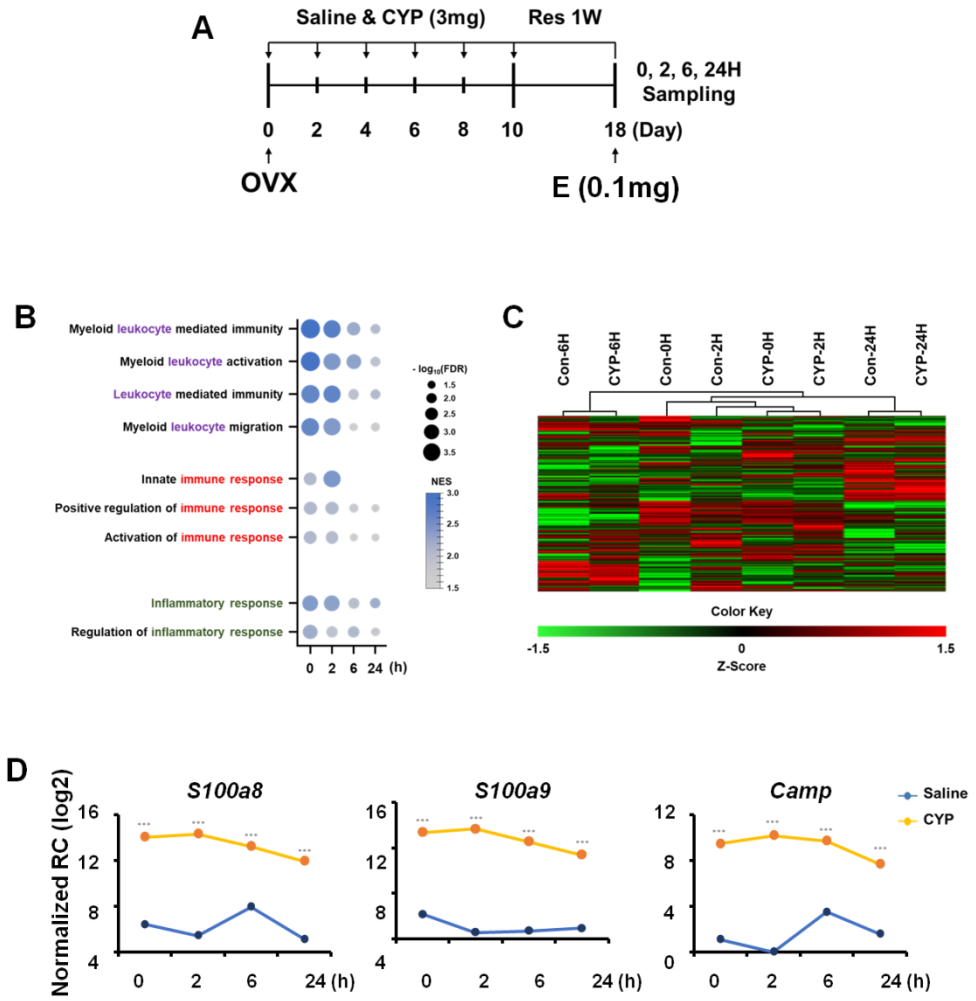

Figure 4. Expression of immune response-related mRNAs in OVX-CYP-one-week-rest model and OVX-saline control after estradiol (E) treatment.

(A) Schedule for 3 mg of CYP or saline (0.1 mL) injection via intraperitoneal (i.p). Injection was performed day 0, 2, 4, 6, 8, and 10 (total six times), and 0.1 mg of E was injected subcutaneously at day 18. And then mice were sacrificed at four time points (0, 2, 6, or 24 hours after E injection).

(B) Gene Ontology enrichment analysis for several upregulated genes in OVX-CYP-1-week-rest at four time points after E injection (relative to OVX-saline control at four time points after E injection). The size and the color of each circle is correlated with the false discovery rate (FDR) values and normalized enrichment score (NES).

(C) Unsupervised hierarchical clustering from GSEA; uterine mRNA expression

profiles in OVX-CYP-1-week-rest and OVX-saline control at four time points after E injection. Gene sets with an FDR q-value < 0.25 (red dotted line) were considered significant.

(D) Expression level of *s100a8*, *s100a9*, and *Cam* throughout four time points by real-time RT-PCR in OVX-CYP-1-week-rest and OVX-saline control (normalized read count, log2) (n = 3-5 per group). Unpaired Student' s t-test, ***p <0.005

Next, uterine expression of several E-responsive mRNAs was investigated. We selected 24 strongly regulated mRNAs by E through previously published literature.[7]

We divided the E-responsive mRNAs into three groups based on the pattern of E-responsiveness, i.e. upregulated, downregulated, and unchanged after E administration.

Fig. 5A shows 17 upregulated E-responsive mRNAs and Fig. 5B shows 8 downregulated E-responsive mRNAs in the OVX-CYP-1-week-rest and OVX-saline control at four time points.

The expression pattern of representative 5 upregulated E-responsive mRNAs (*Bcl7b, Cdkn1a, Cstb, Atf5* and *Pdcd6ip*) was very similar between the OVX-CYP-1-week-rest model and OVX-saline control (Fig. 5C-upper panel).

The expression pattern of representative 4 downregulated E-responsive mRNAs (*Dcn, Serping1, Il15* and *Bach2*) was also very similar between the OVX-CYP-1-week-rest model and OVX-saline control (Fig. 5C-lower panel). These findings can be interpreted that the time-dependent estrogen response pattern was not altered by CYP administration.

When the absolute expression level of each mRNAs was compared between OVX-CYP-1-week-rest and OVX-saline-1-week-rest model at the time point when the expression level of mRNAs was highest, there was significant difference in expression level of *Bcl7b, Cdkn1a, Cstb, Aft5, Dcn, and Serping1* between the two groups.

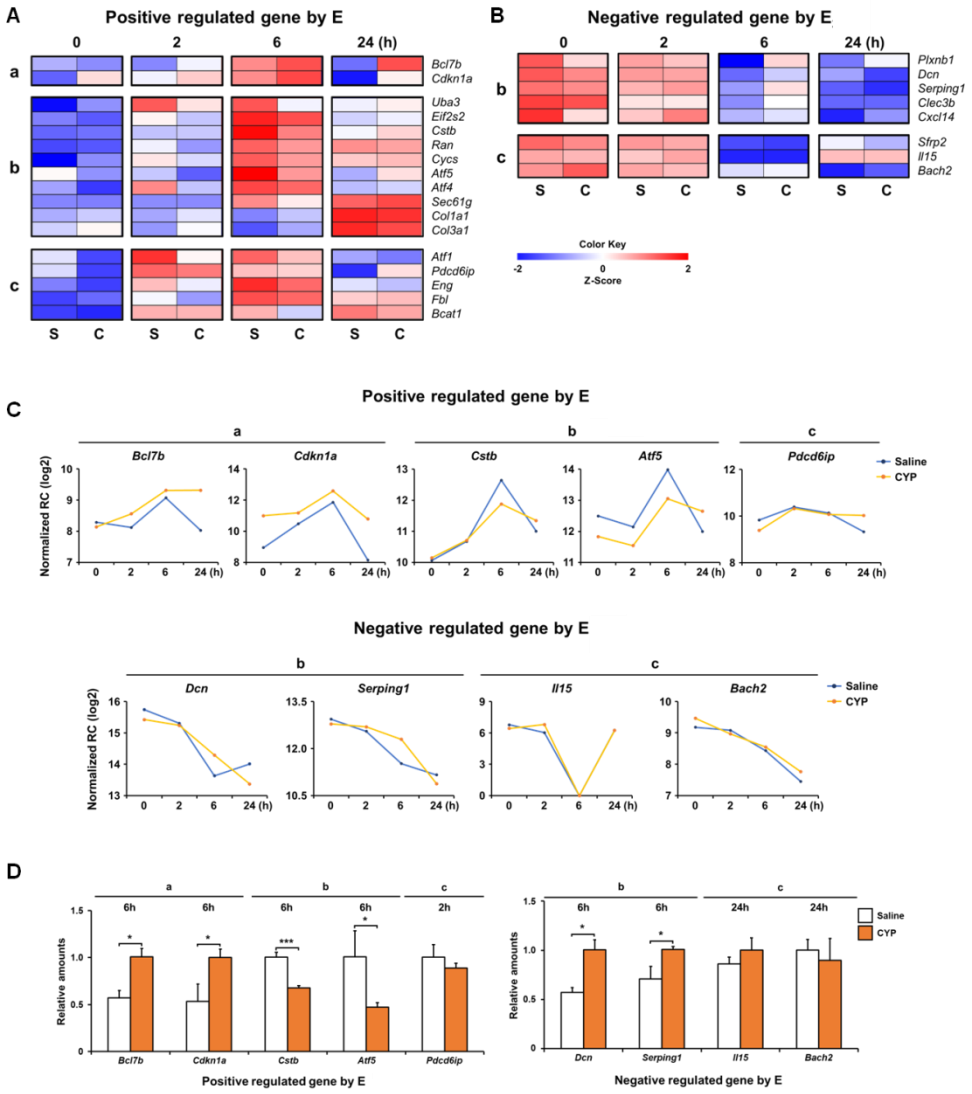

Figure 5. Expression of upregulated or downregulated E-responsive mRNAs in OVX-CYP-one-week-rest model and OVX-saline control after E treatment.

(A) Expression of 17 upregulated E-responsive mRNAs at four time points.

(B) Expression of 8 downregulated E-responsive mRNAs at four time points.

(C) Expression pattern of representative 5 upregulated E-responsive mRNAs (upper panel), and expression pattern of representative 4 downregulated E-responsive mRNAs (lower panel).

(D) Expression level of 5 upregulated E-responsive mRNAs and 4 downregulated

E-responsive mRNAs at specific time points by real-time RT-PCR (normalized read count, log2) (n = 3-5 per group). Unpaired Student' s t-test, *p <0.05, ***p <0.005. a indicates significantly higher expression level in OVX-CYP-one-week-rest model compared to OVX-saline control.

b indicates significantly lower expression level in OVX-CYP-one-week-rest model compared to OVX-saline control.

c indicates similar expression level between OVX-CYP-one-week-rest model and OVX-saline control.

3.5. Expression of immune response-related mRNAs and E-responsive mRNAs in OVX-CYP-two-week-rest model and OVX-saline control after E treatment

Since the expression of immune response-related mRNAs were always higher and the expression of E-responsive mRNAs were quite variable and even markedly altered in the OVX-CYP-one-week-rest model, irrespective of E treatment, we introduced OVX-CYP-two-week-rest model.

In the OVX-CYP-two-week-rest model, 0.1 mg of E was injected subcutaneously at day 24 and then mice were sacrificed at 0, 2, 6, or 24 hours post-E (Fig. 6A).

In the OVX-CYP-two-week-rest model, the body weight nearly recovered at day 24 to similar level with OVX-saline control (Fig. 6B).

The expression level of *s100a8*, *s100a9*, and *Camp* were significantly higher in the OVX-CYP-one-week-rest model, compared to OVX-saline control (as like in former experiment), but their levels (except *Camp*) significantly dropped in the OVX-CYP-two-week-rest model, but those were still significantly higher than OVX-saline control (all were measured at 0-hour post-E) (Fig. 6C).

The expression level of 5 upregulated E-responsive mRNAs became similar between the OVX-CYP-two-week-rest model and

OVX−saline control (Fig. 6D)

The expression level of 4 downregulated E−responsive mRNAs became also similar between the OVX−CYP−two−week−rest model and OVX−saline control (Fig. 6E).

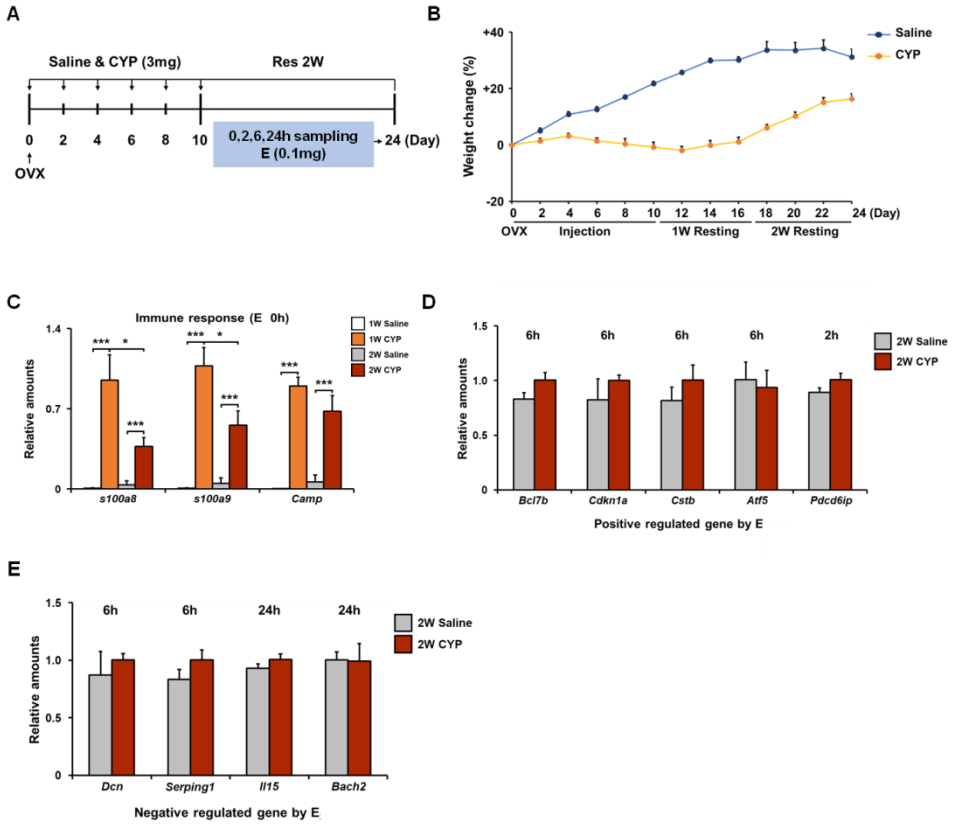

Figure 6. Expression of immune response-related mRNAs and upregulated or downregulated E-responsive mRNAs in OVX-CYP-two-week-rest model and OVX-saline control after E treatment.

(A) Schedule for 3 mg of CYP or saline (0.1 mL) injection via intraperitoneal (i.p). Injection was performed day 0, 2, 4, 6, 8, and 10 (total six times), and 0.1 mg of E was injected subcutaneously at day 24. And then mice were sacrificed at four time points (0, 2, 6, or 24 hours post-E).

(B) Change in percentage of body weight relative to initial body weight on day 1 through day 24 (n = 4 per each group).

(C) Expression level of *s100a8*, *s100a9*, and *Cam* in OVX-CYP-one-week-rest model, OVX-CYP-two-week-rest model, and matched OVX-saline controls by real-time RT-PCR (normalized read count, log2) (n = 4-5 per group). Unpaired Student's t-test, ***p <0.005

(D) Expression level of 5 upregulated E-responsive mRNAs at specific time points in OVX-CYP-two-week-rest model and OVX-saline control by real-time RT-PCR (normalized read count, log2) (n = 4-6 per group).

(E) Expression level of 4 downregulated E-responsive mRNAs at specific time points in OVX-CYP-two-week-rest model and OVX-saline control by real-time RT-PCR (normalized read count, log2) (n = 4-6 per group).

Chapter 4. Discussion

While most researches focused on the gonadal damage after chemo treatment, this study successfully set up an animal model that actualized independent uterine damage by CYP. Using this OVX animal model, we validated that CYP significantly damaged uterine function which was independent from ovarian damage. Specifically, uterine immune response was upregulated after CYP treatment. The expression of E-responsive genes was markedly changed after CYP treatment.

For the first time, as long as we investigated, we showed the ovary-independent uterine damage by CYP in mouse model. The uterus was grossly atrophic after CYP treatment. The functional damage was also validated by showing the lower pregnancy rate, longer time to conceive, and smaller litter size in CYP-treated group compared to the control group.

These findings are consistent with several previous epidemiologic studies showing an increased risk of subfertility and fetal growth restriction in cancer survivors.[8,9]

There can be embryonic and uterine factors explaining the low implantation rate and small litter size after cancer treatment. In the perspective of uterus, the change of endometrial microcirculation after chemo treatment can affect the implantation and placentation.[10,11]

It is well known that chemo agents damage vascular function by

inhibition of vascular endothelial growth factor signaling which causes impaired endothelial function, vascular and renal damage, oxidative stress, and thrombosis.[12]

Verheecke et al. demonstrated that chemotherapy exposure during pregnancy resulted in an increase of oxidative DNA damage and might impact the placental cellular growth and development, resulting in an increased incidence of fetal growth restriction.[11]

Although we did not evaluate the molecular level of endometrial damage by CYP, our results showing atrophic uterus, lower pregnancy rate and smaller litter size in CYP group support these previous researches suggesting an impaired placentation after chemo treatment.

Of note, we used ovariectomized mice to evaluate uterine damage independent from ovarian damage by CYP. In ovariectomized mice, immune response related gene expression was up-regulated in CYP group compared to control group.

Specifically, the expression of *S100a8/9* was significantly increased in CYP group. *S100a8/9*, also known as calprotectin, are heterodimeric EF-hand Ca^{2+} binding proteins and involved in inflammatory process.[13]

Elevated levels of *S100a8/9* were detected in inflammation, neoplastic tumor cells and various human cancers. Also, in inflammatory responses in peripheral tissues, *S100a8* is a potent chemoattractant and also an anti-oxidant which are important roles in

placenta development.[13]

It was reported that overexpression of *S100a8/9* might increase the recruitment of inflammatory leukocytes in maternal–fetal interface resulting in utero–placental perfusion deficiency, development of thrombotic events, and placental hypoxia, eventually embryo abortion.[14]

Based on these previous reports, our results might show that increased expression of *S100a8/9* by CYP treatment has a detrimental effect on uterine function which would lead to lower pregnancy rate, longer time to conceive and smaller litter size. This may be a target of future researches which focus on developing treatment modality to improve uterine function after chemo treatment.

Cyclic AMP (cAMP) is known to mediate decidualization of human endometrial stroma and gland development.[15] It triggers intracellular signaling pathways that affect diverse downstream molecules. It has been documented that decidualization is mainly regulated by both protein kinase A (PKA) and exchange protein directly activated by CAMP signalings.[16]

These data reveal that cAMP is a key mediator of decidualization in ESCs. Activation of the cAMP signaling increases cyclooxygenase (COX) 2 expression in endometrial glandular cells.[16]

However, there is no study reporting how supraphysiologic level of CAMP affects on the endometrial function and decidualization. In our

study, CYP treated uterus had significantly increased level of cAMP gene expression. Further studies are warranted about the optimal expression level of CAMP in uterus for decidualization.

Frozen gametes are usually transferred into uterus which is pre-treated with ovarian steroid hormonal (E and progesterone) to mimic the secretory phase endometrium. Endometrial E response is a key factor for a successful implantation.

We validated that the expression of uterine E response genes was significantly altered after CYP treatment compared to control group. Especially, we found that immune and uterine E response is also dependent on the resting period after chemo treatment. Interestingly, 2 weeks of resting period after CYP administration, the difference in the expression of uterine E response genes between the two groups, which was remarkable after 1 week of resting, was markedly decreased.

When we compared the expression level of *S100a8/9* and *Camp* after 1 week and 2 weeks of resting period, the up-regulation of the expression of these genes is markedly decreased after 2 weeks of resting period.

It is a clinically important finding because, in the era of fertility preservation, to validate the optimal period to use the frozen gametes is the key factor for a successful pregnancy. However, there is a lack of previous literature and still no consensus about the optimal timing to try to conceive after breast cancer treatment.

In that sense, our finding suggests a scientific evidence supporting that sufficient resting period after chemo treatment should be preceded to restore the uterine damage.

Further studies are warranted to investigate the optimal resting period to try to conceive after breast cancer chemo treatment in human.

Our study has several strengths and limitations. Most of all, this is the first animal model study evaluating the CYP impact on uterus independent from ovary. In addition, we validated the possible mechanism of uterine damage by CYP which can be a target of therapy in the future.

Also, by providing experimental data indicating that uterine recovery after cancer treatment is time-dependent, our study guided future studies which are warranted to validate optimal implantation period after the cessation of cancer treatment in human.

The biggest limitation of our study is that, because this is an animal study, further human studies are needed to find the clinical application of our results. In clinical settings, it would be more complex because of the variety of chemo protocols. Finally, we failed to consider the role of progesterone which is critical in decidualization.

This is the first study looking at the independent uterine damage by CYP in mice model. The uterine E response was also altered after CYP treatment. It is important that the damage was shown to be

reversible by resting. Further human studies are warranted to aid cancer survivors plan to start to conceive after the cessation of cancer treatment.

References

1. Kim J, Oktay K, Gracia C, et al: Which patients pursue fertility preservation treatments? A multicenter analysis of the predictors of fertility preservation in women with breast cancer. Fertil Steril 97:671-6, 2012

2. Kim J, Turan V, Oktay K: Long-Term Safety of Letrozole and Gonadotropin Stimulation for Fertility Preservation in Women With Breast Cancer. J Clin Endocrinol Metab 101:1364-71, 2016

3. Oktay K, Turan V, Bedoschi G, et al: Fertility Preservation Success Subsequent to Concurrent Aromatase Inhibitor Treatment and Ovarian Stimulation in Women With Breast Cancer. J Clin Oncol 33:2424-9, 2015

4. Vernaeve V, Bodri D, Colodron M, et al: Endometrial receptivity after oocyte donation in recipients with a history of chemotherapy and/or radiotherapy. Hum Reprod 22:2863-7, 2007

5. Hartnett KP, Mertens AC, Kramer MR, et al: Pregnancy after cancer: Does timing of conception affect infant health? Cancer 124:4401-4407, 2018

6. Liani-Leibson K, Har-Vardi I, Priel E: Inhibition of topoisomerase I by anti-cancer drug altered the endometrial cyclicity and receptivity. Curr Mol Med 14:141-50, 2014

7. Quinlan AR, Hall IM: BEDTools: a flexible suite of utilities for comparing genomic features. Bioinformatics 26:841-2, 2010

8. Madanat-Harjuoja LM, Malila N, Lahteenmaki PM, et al: Preterm delivery among female survivors of childhood, adolescent and young adulthood cancer. Int J Cancer 127:1669-79, 2010

9. Stensheim H, Klungsoyr K, Skjaerven R, et al: Birth outcomes among offspring of adult cancer survivors: a population-based study. Int J Cancer 133:2696-705, 2013

10. Kruger-Genge A, Steinbrecht S, Kupper JH, et al: Evidence for cytostatic effect of cyclophosphamide on human vein endothelial cells in cancer therapy: Preliminary in vitro results. Clin Hemorheol Microcirc 69:267-276, 2018

11. Verheecke M, Cortes Calabuig A, Finalet Ferreiro J, et al: Genetic and microscopic assessment of the human chemotherapy-exposed placenta reveals possible pathways contributive to fetal growth restriction. Placenta 64:61-70, 2018

12. Cameron AC, Touyz RM, Lang NN: Vascular complications of cancer chemotherapy. Can J Cardiol 32:852-62, 2016

13. Baker JR, Jeffery R, May RD, et al: Distinct roles for S100a8 in early embryo development and in the maternal deciduum. Dev Dyn 240:2194-203, 2011

14. Shabani F, Farasat A, Mahdavi M et al: Calprotectin (S100A8/S100A9): a key protein between inflammation and cancer. Inflamm Res 67:801-812, 2018

15. Kazuya K, Mikihiro Y, Kazuhiro T, et al: Regulatory action of

calcium ion on cyclic AMP-enhanced expression of implantation related factors in human endometrial cells. PLoS One 10:1-17, 2015

16. Zhou XL, Lei ZM, Rao CV: Treatment of human endometrial gland epithelial cells with chorionic gonadotropin/luteinizing hormone increases the expression of the cyclooxygenase-2 gene. J Clin Endocrinol Metab 84: 3364-3377, 1999

국문 초록

목적: 본 연구에서는 항암치료제인 사이클로포스파마이드의 자궁 독성을 규명하고 그 회복 기전 및 임상적 치료법을 쥐 실험을 통해 분석하고자 하였다.

방법: 7주령 C57BL/6 암컷 쥐의 복강에 2일 마다 총 6회에 걸쳐 사이클로포스파마이드 3 mg을 투약하였다. 생리식염수 투약군을 대조군으로 하였다. 실험1에서는, 실험 11일째에 쥐를 희생시켜 주요 기관들의 형태학적, 조직학적 변화를 관찰하였다. 생식능 변화를 관찰하기 위해 실험 16일째에 수컷쥐와 교배시켜 임신 여부를 확인하였다.

실험2에서는 난소를 제거한 암컷 쥐에 같은 프로토콜로 사이클로포스파마이드를 투여하고 투여 종료 1주와 2주 후에 에스트라디올 0.1 mg을 피하 주입하였다. 에스트라디올 투여 0, 2, 6, 24 시간 후 쥐를 희생시켜 자궁 조직을 채취하여 RNA-seq, reverse transcription-PCR (RT-PCR), 및 real-time RT-PCR 분석을 하였다.

결과: 실험1에서는 사이클로포스파마이드 투약군의 자궁은 심하게 위축되었으며 난소 크기 또한 대조군에 비해 줄어들었다. 난포 개수도 사이클로포스파마이드 투약 군에서 현저히 줄어들었다. 교배 후 플러그 형성까지 걸리는 시간이 사이클로포스파마이드 투약 군에서 유의하게 길게 나타났고 임신율 및 새끼 크기 모두 사이클로포스파마이드 군에서 낮았다.

실험2에서는 난소제거-사이클로포스파마이드-1주 휴지기 군에서는

자궁내막의 면역 관련, 세포사 및 스트레스 반응 관련 유전자 발현이 유의하게 증가된 소견을 보였으며 이러한 반응은 에스트로겐 투여와는 무관하였다. 그러나 이렇게 증가된 발현량은 난소제거-사이클로포스파마이드-2주 휴지기 군에서는 감소하여 대조군과 비슷한 발현량을 나타냈다. 에스트로겐 반응성 유전자 발현은 난소제거-사이클로포스파마이드-1주 휴지기 군에서는 매우 다양한 양상으로 변하였으며 역시 에스트로겐 투여와는 무관하였다. 그러나 이렇게 다양하게 변화한 발현량은 난소제거-사이클로포스파마이드-2주 휴지기 군에서는 대조군과 비슷하게 되었다.

결론: 사이클로포스파마이드 투여 후 쥐의 자궁과 내막은 위축되었고 난포 개수는 저하되었으며, 가임능도 현저히 손상되었다. 난소를 제거한 쥐에 사이클로포스파마이드를 투여하고 1주 후에 자궁을 보았을 때 다양한 유전자가 변화하였으나 이러한 변화는 에스트로겐 투여로는 호전이 없고 대신 2주 휴지기 후에는 유전자 발현 변화가 현저히 줄어든 것으로 보아 사이클로포스파마이드 투여에 의한 자궁 유전자 발현 변화는 2주 휴지기를 거침으로써 정상화될 수 있다고 사료된다.

주요어: 사이클로포스파마이드; 난소; 가암력; 자궁; 자궁내막; 에스트로겐

학 번: 2015-30567